SIOG 231
GEOMAGNETISM AND ELECTROMAGNETISM

Lecture 15
Magnetohydrodynamics in Earth's Core II
2/27/2024

Background reading: Chapter 3 of Earth's Core, by Cormier et al., 2022
https://doi.org/10.1016/B978-0-12-811400-1.00004-5

Today's Class

- Reminder that the MagnetoHydroDynamics (MHD) approximation gives us the magnetic induction equation for changing magnetic field in Earth's core
- Look at 2 end member cases - i. diffusive decay; ii. the frozen flux approximation (FFA)- FFA provides us with properties that are invariant with time and lets us look (in part) at surface flow in Earth's core.
- In between case allows interaction between poloidal and toroidal fields that are essential to dynamo operation.
- Numerical dynamo simulation lets us look in detail inside the core if we can predict the flow $\mathbf{u}$. Need a force balance equation.
- An example of merging numerical dynamo simulations with initial condition from field modeling to infer gyre driven geomagnetic decay of Earth's dipole

Recall the magnetic induction equation describing temporal changes in B for the geodynamo

$$\frac{\partial \mathbf{B}}{\partial t} = \nabla \times (\mathbf{u} \times \mathbf{B}) + \eta \nabla^2 \mathbf{B}$$

with $\eta = \dfrac{1}{\mu_o \sigma}$, the magnetic viscosity analogous to kinetic viscosity in ordinary fluid flow.

The two terms on the RHS correspond to advection and diffusion and we will explore end member scenarios in which each one of them is dominant.

Recall that estimates for η range from 0.4 -2.0 m^2/s

Recall the magnetic induction equation describing temporal changes in B for the geodynamo

$$\frac{\partial \mathbf{B}}{\partial t} = \underbrace{\boxed{\nabla \times (\mathbf{u} \times \mathbf{B})}}_{\text{advection}} + \underbrace{\boxed{\eta \nabla^2 \mathbf{B}}}_{\text{diffusion}}$$

with $\eta = \dfrac{1}{\mu_o \sigma}$, the magnetic viscosity - analogous to kinetic viscosity in ordinary fluid flow.

The two terms on the RHS correspond to advection and diffusion and we will explore end member scenarios in which each one of them is dominant.

Magnetic Reynolds Number in the Core

- Recall from our hypothetical dynamo that Rm is the ratio of two time scales: the magnetic diffusion time $\tau_{mag} = d^2/\eta$ and the circulation or overturn time $\tau_{circ} = d/v$.

- Let's assume that in Earth's core,
  the velocity field has a characteristic magnitude *U;*
  magnetic field has characteristic magnitude *B;*
  length scale over which field changes is *L.*
- Then the ratio of the terms on the RHS of the induction equation will be

$$\frac{|\nabla \times (u \times \mathbf{B})|}{\eta \nabla^2 \mathbf{B}} = \frac{UB/L}{\eta B/L^2} = \frac{\tau_{mag}}{\tau_{circ}} = \frac{UL}{\eta} = \mu_0 \sigma UL = Rm$$

For global motion in Earth's core we can take L as outer core thickness (2260 km), U~ *2* mm/s, $\eta \sim 1$, then Rm ~ 4000, easily larger than the critical value for dynamo action (~ 40). Earth's dynamo is strongly supercritical.

Diffusion of the Magnetic Field-1

- Sustaining the geomagnetic field requires some balance between the advection and diffusion terms in the geomagnetic induction equation. Let's look at these individually.

- We start with $\frac{\partial \mathbf{B}}{\partial t} = \eta \nabla^2 \mathbf{B}$ (corresponding to low *Rm*). Without fluid flow we expect the field will decay over time from its initial amplitude $\mathbf{B}_0$ with characteristic decay time t_0. In a simple plane wave this would look like:

  $\mathbf{B}(x, t) = \mathbf{B_0} e^{2\pi i x} e^{-t/t_0}$

  We need the solution in a sphere for both poloidal and toroidal parts of the field. Fortunately in the low *Rm* limit there is no interaction between them.

Diffusion of the Magnetic Field -2

Recall the poloidal/toroidial decomposition of the field (Slide 11, Lecture 14)

$$\mathbf{B} = \nabla \times (T\mathbf{r}) \; + \; \nabla \times \nabla \times (P\mathbf{r}) = \mathbf{B}_T \; + \; \mathbf{B}_P$$

When Rm is small each scale potential obeys its own diffusion equation, and the toroidal and poloidal field scalars will diffuse independently.

$$\frac{\partial T}{\partial t} = \eta \nabla^2 T \qquad\qquad \frac{\partial P}{\partial t} = \eta \nabla^2 P$$

Slowest decay term in P is the dipole and for a core of uniform conductivity we find the solution in a sphere of radius c involves the spherical Bessel function order 1, j_1, and

$$P(t) = P_0 j_1(\pi r/c) \cos\theta (e^{-t/t_{dip}})$$

with dipole decay time $\tau_{dip} = \dfrac{c^2}{\pi^2 \eta} \sim$ 20-50 ky for η corresponding to current views of core conductivity.

Dipole moment in free decay obeys an equation like that for P, so $\mathbf{m} = \mathbf{m_0} e^{-t/\tau_{dip}}$.

This verifies we really do need a mechanism to continually regenerate the geomagnetic field for it to survive for several Ga.

Now lets look at pure advection - just fluid flow

- Consider the case in which the second term on the right hand side is negligible (i.e. perfect conductivity), then

$$\frac{\partial \boldsymbol{B}}{\partial t} = \nabla \times (\boldsymbol{u} \times \boldsymbol{B})$$

Alfvén's theorem:
Magnetic field lines move with a perfectly conducting fluid as though frozen to it.

Using the standard vector calculus relation,

$$\nabla \times (\boldsymbol{u} \times \boldsymbol{B}) = (\boldsymbol{B} \cdot \nabla) \boldsymbol{u} - (\boldsymbol{u} \cdot \nabla) \boldsymbol{B} \quad \text{since} \quad \nabla \cdot \boldsymbol{u} = 0 \quad \text{and} \quad \nabla \cdot \boldsymbol{B} = 0$$

$$\frac{\partial \boldsymbol{B}}{\partial t} + (\boldsymbol{u} \cdot \nabla) \boldsymbol{B} = (\boldsymbol{B} \cdot \nabla) \boldsymbol{u} \quad \text{or} \quad \frac{D \boldsymbol{B}}{Dt} = (\boldsymbol{B} \cdot \nabla) \boldsymbol{u}$$

Advection of magnetic field along with flow

Stretching of magnetic field by shear of flow

Now consider a material patch of outer core fluid with surface area A oriented by a normal unit vector $\hat{\mathbf{n}}$.

The total magnetic flux Φ must obey the important condition

$$\frac{d\Phi}{dt} = \frac{d}{dt}\int(\mathbf{B}\,.\,\hat{\mathbf{n}})dA = 0 \text{ Alfvén's Theorem}$$

Total magnetic flux within the path is conserved in time. Magnetic flux moves as though frozen into the conductor.

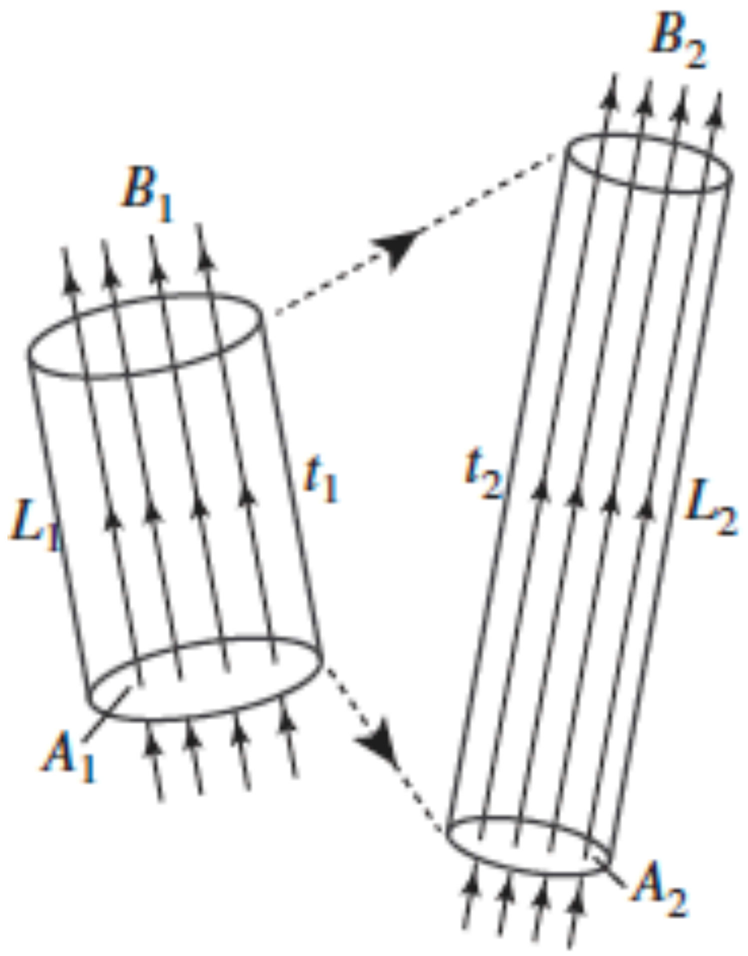

FIG. 3.17 Illustration of magnetic field intensification by fluid motion in the frozen flux (perfect conductor) limit. Stretching of an incompressible perfectly conducting cylinder containing magnetic flux $\Phi = A_1B_1$ at t_1 and conserves Φ at t_2 but intensifies the magnetic field according to $B_2/B_1 = L_2/L_1 = A_1/A_2$.

Shape of the contour evolves with time but the total flux is invariant.

Perfect Conductivity: Frozen Flux

$$\frac{d}{dt}\int_S \boldsymbol{B}\cdot d\boldsymbol{S} = \int_S \frac{\partial \boldsymbol{B}}{\partial t}\cdot d\boldsymbol{S} + \oint_C \boldsymbol{B}\cdot\boldsymbol{u}\times d\boldsymbol{l} =$$

$$= \int_S \frac{\partial \boldsymbol{B}}{\partial t}\cdot d\boldsymbol{S} - \oint_C \boldsymbol{u}\times\boldsymbol{B}\cdot d\boldsymbol{l}$$

$$= \int_S \left(\frac{\partial \boldsymbol{B}}{\partial t} - \nabla\times(\boldsymbol{u}\times\boldsymbol{B})\right)\cdot d\boldsymbol{S} = 0$$

The total flux enclosed by a material surface cannot change with time even if the shape of the contour evolves : FLUX IS FROZEN

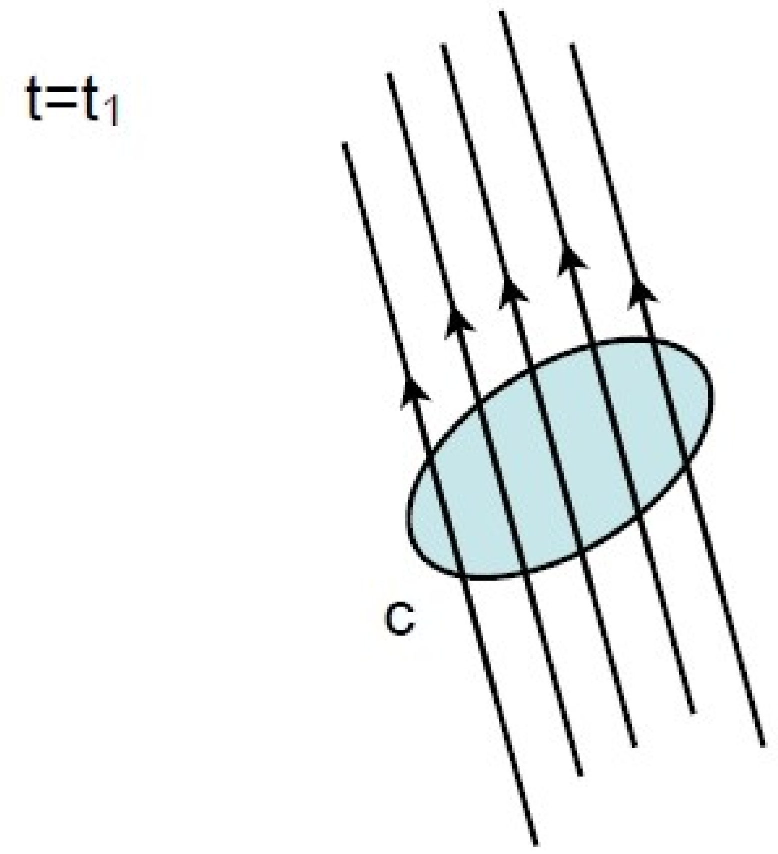

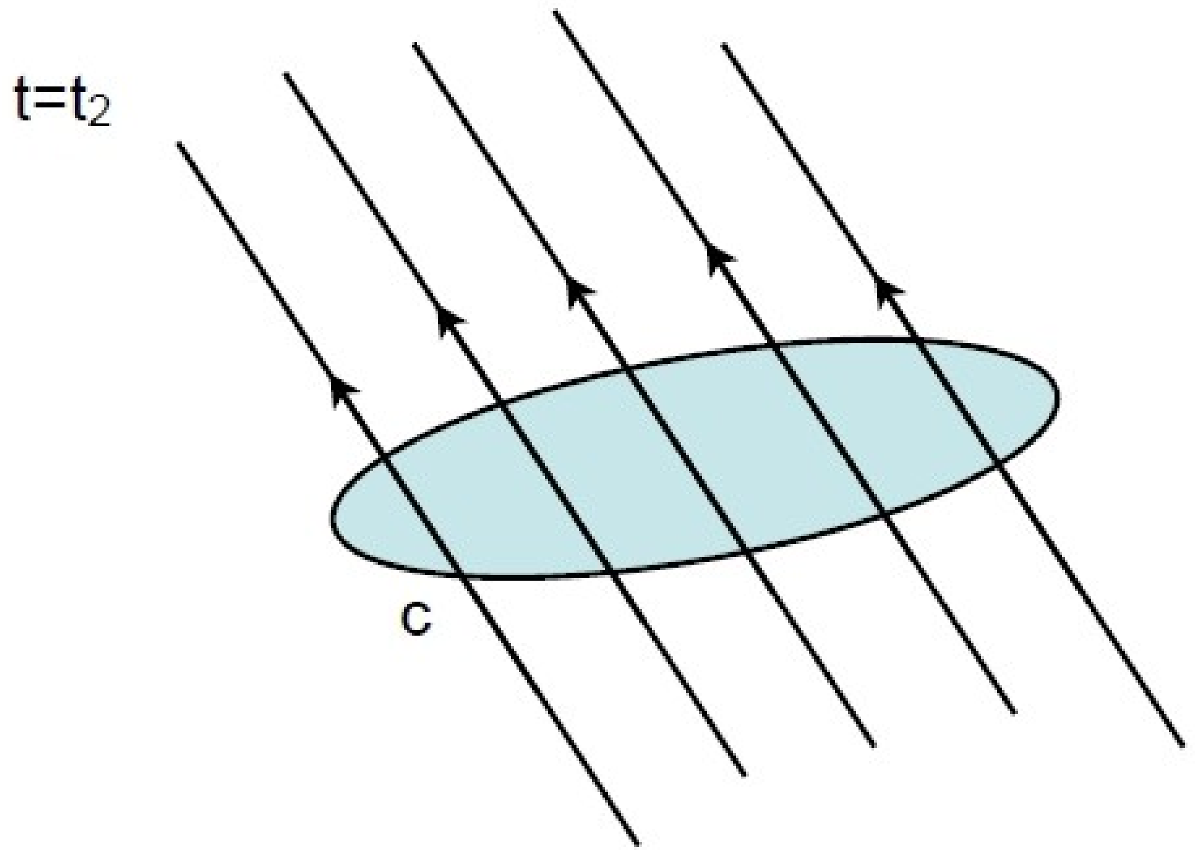

Why is this at all useful?
If can identify patches on the core surface maybe we can detect Ohmic diffusion.

Frozen-flux approximation is the starting point for attempts to map fluid flow at the core surface.

Does the Frozen Flux Approximation (FFA) work?

Number of null flux curves and integral of B_r through each should remain constant over time. This can be tested if our maps of B_r at the CMB are sufficiently accurate.

gufm1 field model at Core-mantle Boundary

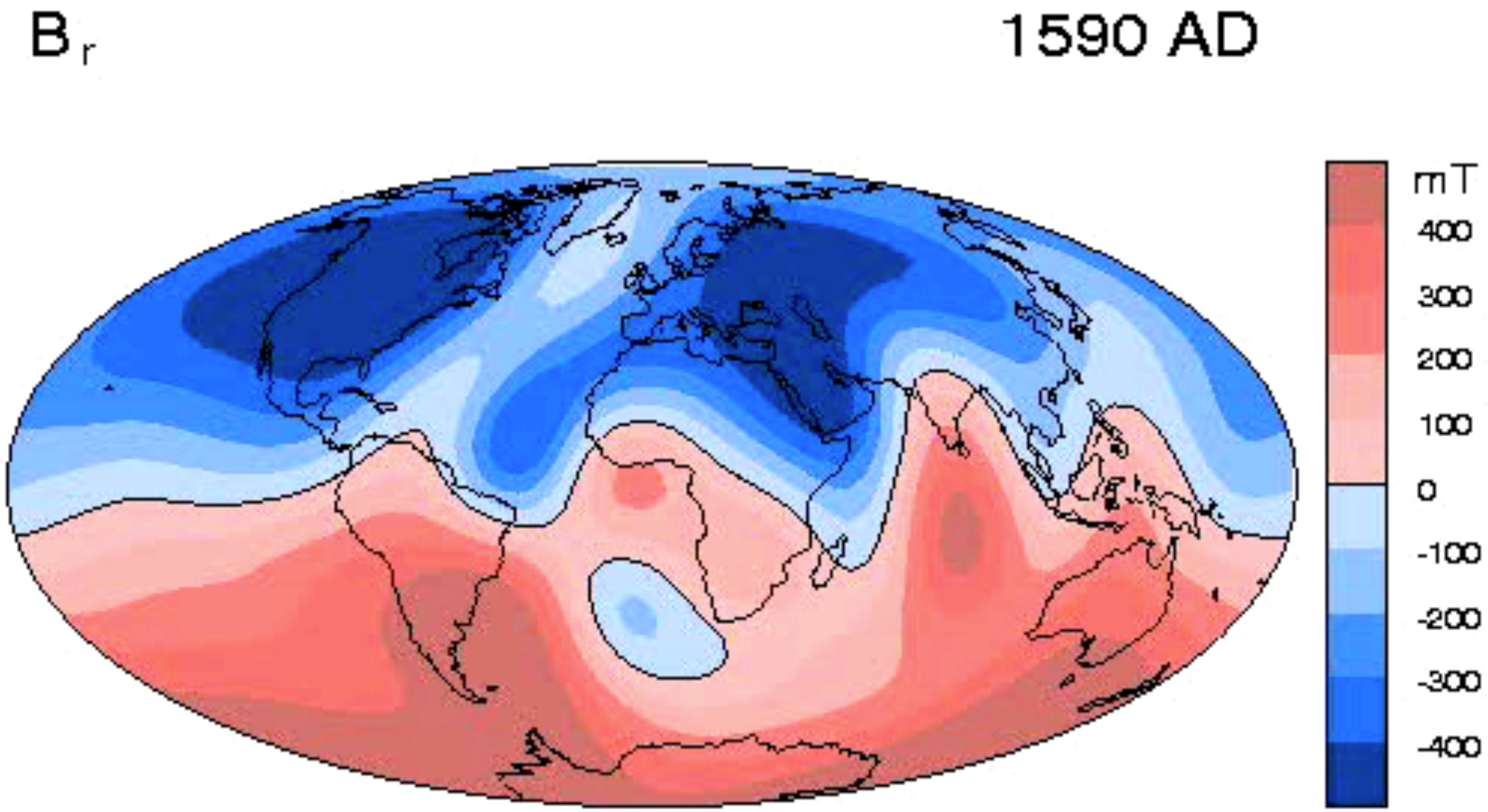

FFA relies on high *Rm* and ability to ignore magnetic diffusion. We expect this to be a better approximation at large spatial scales and over short time intervals.

Tracking core surface flow under FFA

In the perfect conductor limit of the induction equation (no magnetic diffusion)

$$\frac{\partial \mathbf{B}}{\partial t} + (\mathbf{u} \cdot \nabla)\mathbf{B} = (\mathbf{B} \cdot \nabla)\mathbf{u}$$

For the radial component of the rate of magnetic change just below the CMB we can write a tracer equation for B_r

$$\frac{\partial B_r}{\partial t} + (\mathbf{u}_H \cdot \nabla)B_r = -B_r(\nabla_H \cdot \mathbf{u})$$

where the H refers to the horizontal component of the flow and we have supposed that the radial component of **u** can be neglected (fluid can't pass through the CMB).

Tracking core surface flow under FFA

In the perfect conductor limit of the induction equation (no magnetic diffusion)

$$\frac{\partial \mathbf{B}}{\partial t} + (\mathbf{u} \cdot \nabla)\mathbf{B} = (\mathbf{B} \cdot \nabla)\mathbf{u}$$

For the radial component of the rate of magnetic change just below the CMB we can write a trace equation for B_r

$$\frac{\partial B_r}{\partial t} + \underbrace{\boxed{(\mathbf{u}_H \cdot \nabla)B_r}}_{\text{advective transport}} = \underbrace{\boxed{-B_r(\nabla_H \cdot \mathbf{u})}}_{\text{Intensity changes in Br due to horizontal divergence of outer core flow}}$$

where the H refers to the horizontal component of the flow and we have supposed that the radial component of $\mathbf{u}$ can be neglected. If we know B_r and $\frac{\partial B_r}{\partial t}$ it is possible to recover $\mathbf{u}_H$ provided we supply some additional constraints to resolve the two horizontal velocity components..

Calculation of Fluid Flow Models at the Surface of the Core

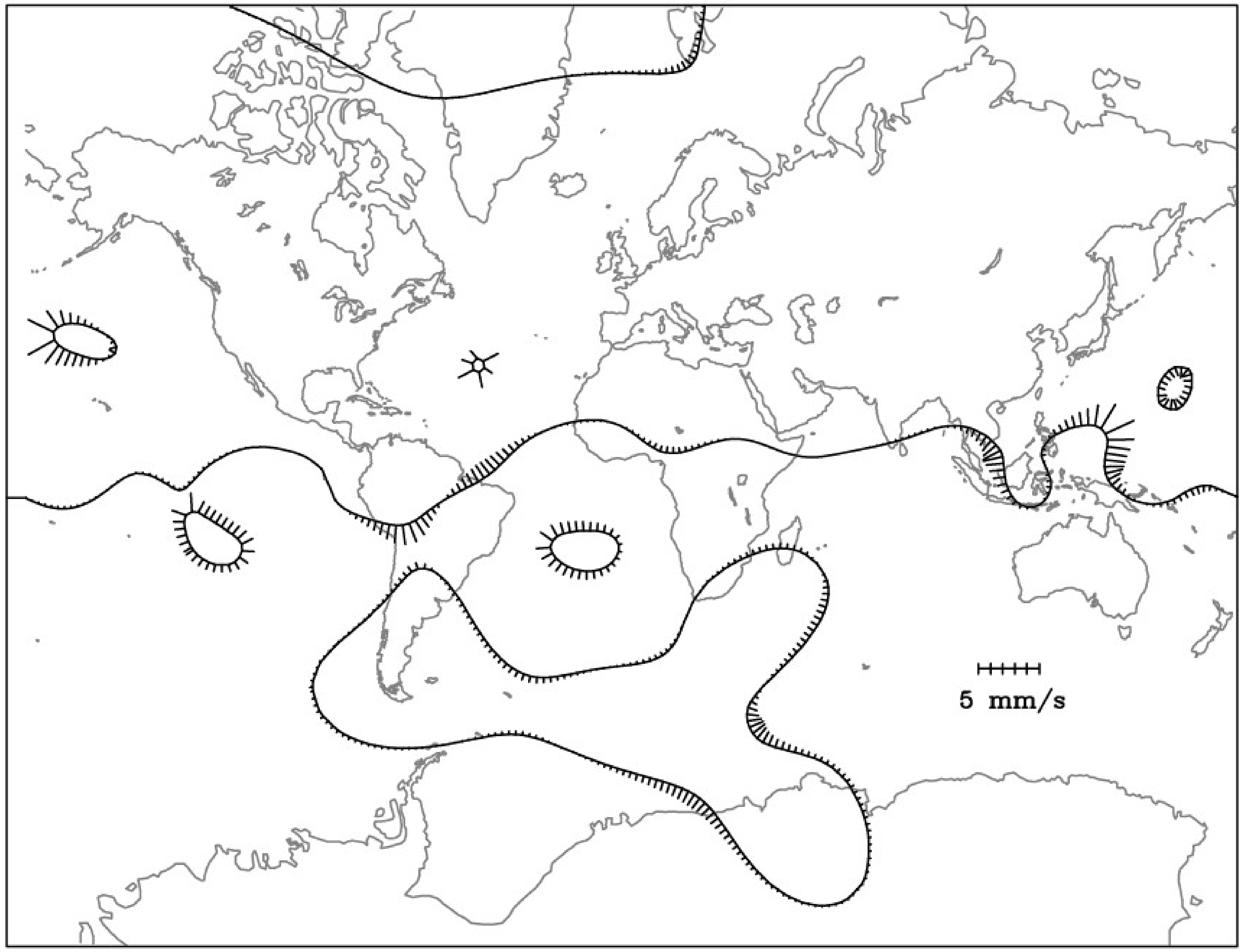

Core surface velocity **orthogonal to null flux curves** (places where $B_r = 0$) in IGRF 1980. These velocities can be determined uniquely from the positions of the null flux curves if they are known.

Components parallel to the curves are unknown, because $\nabla_H \cdot \mathbf{u} = 0$ parallel to B_r contours, and under FFA there is no secular variation there.

Additional constraints used to recover both components of $\mathbf{u}_H$ everywhere under FFA could be:

- steady state flow
- purely toroidal flow
- tangentially geostrophic or quasi-geostrophic
- columnar flow
- helical flow.

What do the additional constraints mean?

- steady state - no change in $\mathbf{u}$ with time

- toroidal flow - horizontal divergence of velocity, $\nabla_H \cdot \mathbf{u} = 0$ or $u_r = 0$ - reasonable if expect stable stratification in E' layer of outer core

- tangential geostrophy - geostrophic force balance to tangential components of flow leads to $\nabla_H \cdot (\mathbf{u} \cos\theta) = 0$

- columnar flow constraint - $\nabla_H \cdot \mathbf{u} = \dfrac{2\tan\theta}{c} u_\theta$

- helical flow assumes tangential divergence of the flow, $\nabla_H . \mathbf{u}$, is spatially correlated with the radial component of the vorticity $(\nabla \times \mathbf{u})_r$ - expect this for α^2 dynamo and strongly helical flow due to influence of Coriolis acceleration

FF image of flow near top of core with columnar constraint

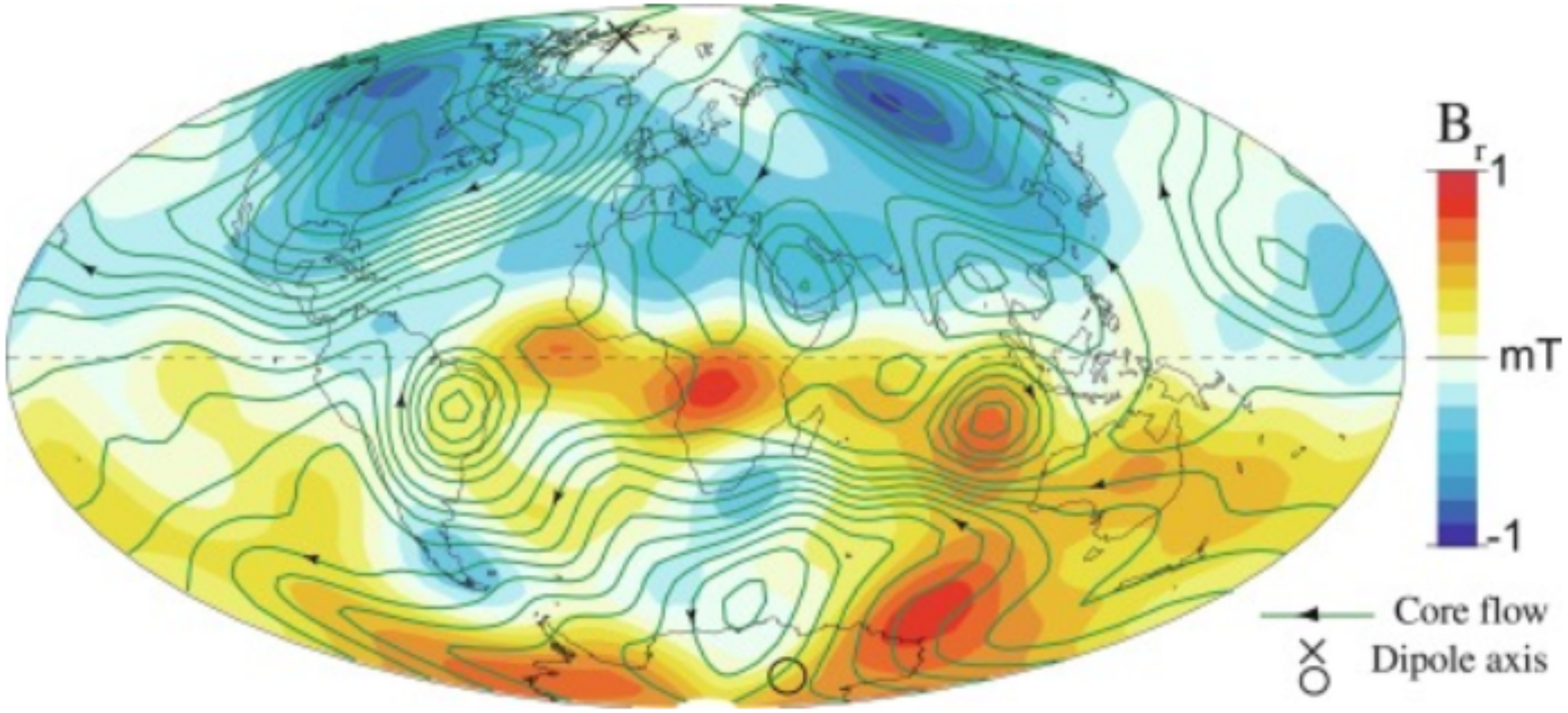

Note the large counterclockwise gyre in the southern hemisphere beneath the southern ocean, high latitude vortices around the intense flux patches. These are common to almost all frozen flux inversions.

Download : Download full-size image

Fig. 3.25. A frozen flux image of flow near the top of the outer core at epoch 2005 based on the columnar flow constraint. Streamlines of the horizontal flow with *directional arrows* are shown overlaying contours of the radial magnetic field on the core-mantle boundary at the same epoch. Continental outlines are shown for reference. *Black cross* and *circle* denote the location of the North and South Geomagnetic Poles, respectively.

Independent Checks on FFA

Length of day variations predicted from core flow - due to changes in angular momentum in the core transmitted to the mantle.

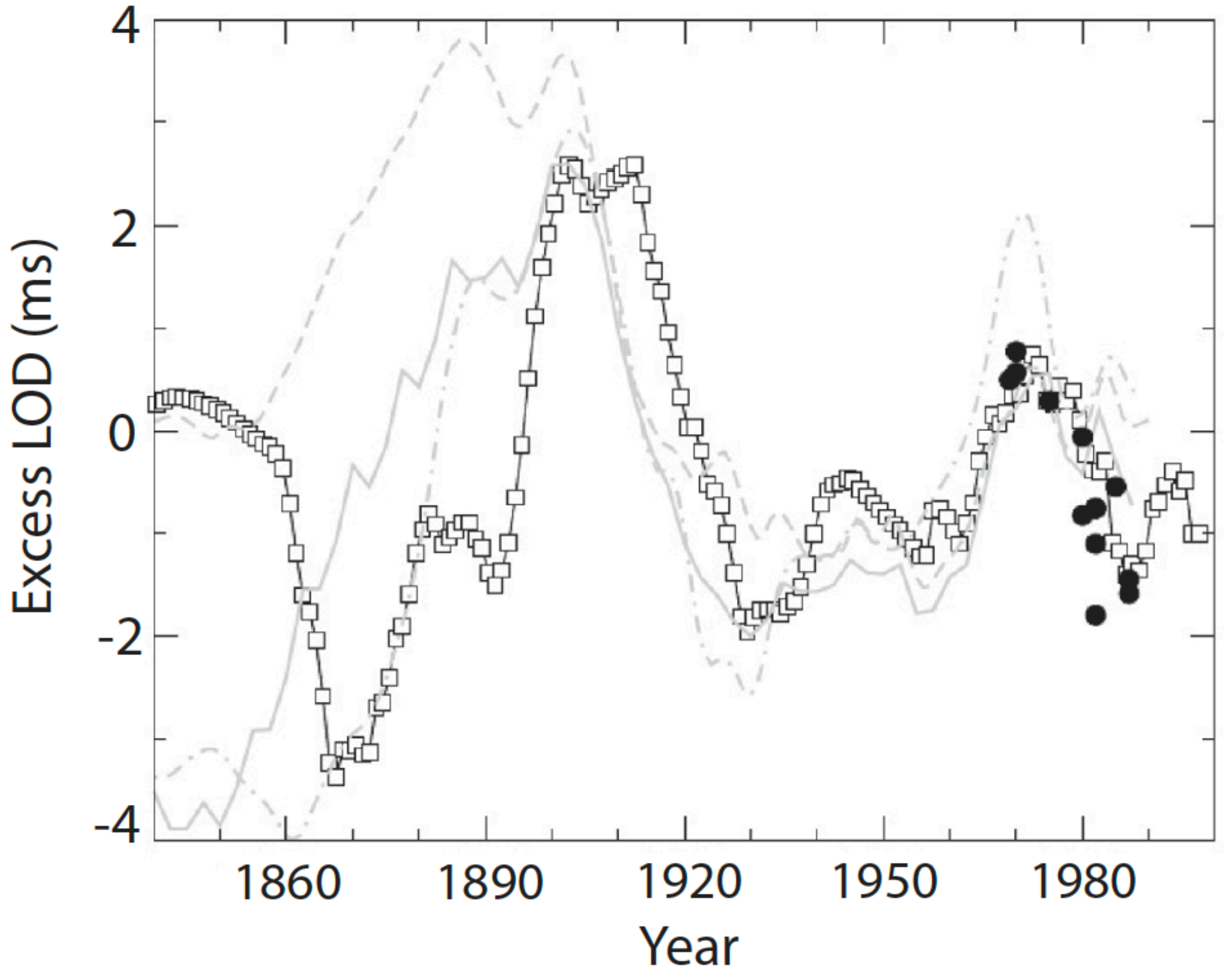

FIG. 3.26 Comparison of the observed excess length-of-day variations (in milliseconds) that is attributed to the deep Earth (*squares and filled circles*), with predictions from various frozen flux images of core flow. *Reproduced with permission from Ponsar, S., Dehant, V., Holme, R., Jault, D., et al., 2003. The core and fluctuations in the Earth's rotation. In: Dehant, V., Karato, S., Zatman, S. (Eds.), Earth's Core: Dynamics, Structure, Rotation. AGU Geodynamics Series v31.*

Back to the full induction equation and the in-between case of finite but large *Rm*

Poloidal, *P,* and toroidal, *T,* potentials and fields will interact. In terms of radial field and velocity, B_r, u_r respectively, with $ru_r = \mathbf{r} \cdot \mathbf{u}$ it can be shown that

$$\frac{\partial}{\partial t} rB_r + (\mathbf{u} \,.\, \nabla) rB_r = \eta \nabla^2 rB_r + (\mathbf{B_T} + \mathbf{B_P}) \cdot \nabla (ru_r), \qquad **$$

where

$$rB_r = \mathbf{r} \,.\, \mathbf{B} = \mathbf{r} \cdot \nabla \times \nabla \times (\mathbf{r}P).$$

** can be thought of as being like a heat transport equation for poloidal field, with the 2nd term on the RHS a magnetic field production term involving both toroidal and poloidal terms. There is a similar equation for the toroidal field.

Poloidal field is transported and diffuses much like temperature, but production is proportional to both potentials and also to the fluid radial velocity. Coupling can amplify the poloidal field through interaction with fluid $\boldsymbol{u}$. Note that when $u_r = 0$ there is no coupling.

Radial fluid motion is needed to generate the poloidal magnetic field in the core. Horizontal motions are not sufficient, although they do affect the field structure.

We started with

Ingredients needed for a dynamo

- large electrically conducting fluid in planetary interior
- energy supply (for convection)
- planetary rotation (swirls the field around)

Additional needs for dynamo regeneration

- supercritical Magnetic Reynolds number, *Rm*
- fluid motion with helicity to produce an α effect
- fluid motion with shear for ω-effect
- Ohmic dissipation contributes much more to energy loss than viscous friction, so kinetic/ magnetic energy exchange is extremely important.

Energy Pathways in self-sustaining dynamo system

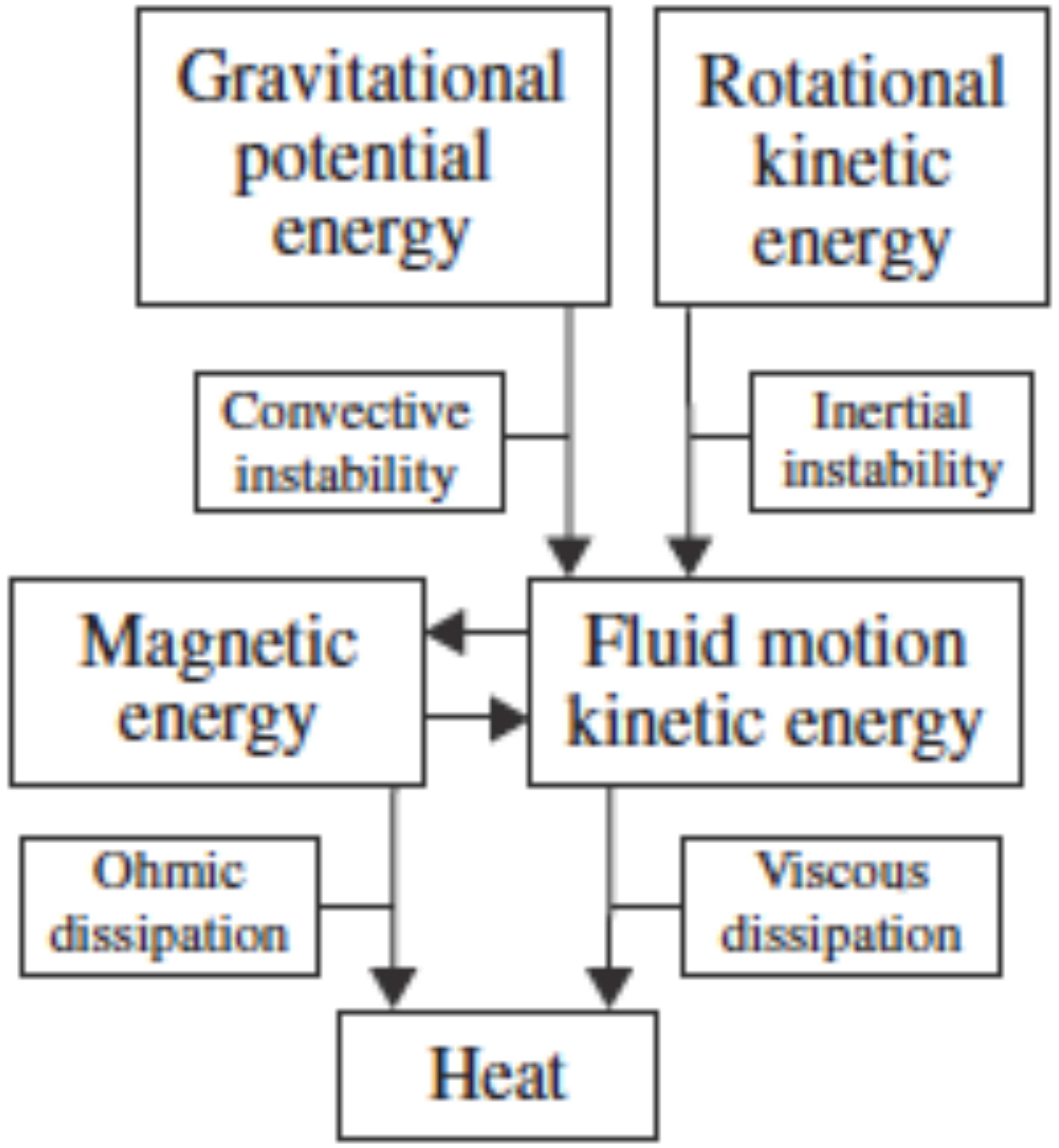

Figure 3.24, Earth's Core

Then alpha effect drives helicity from overall rotation

3.3 The geodynamo process 99

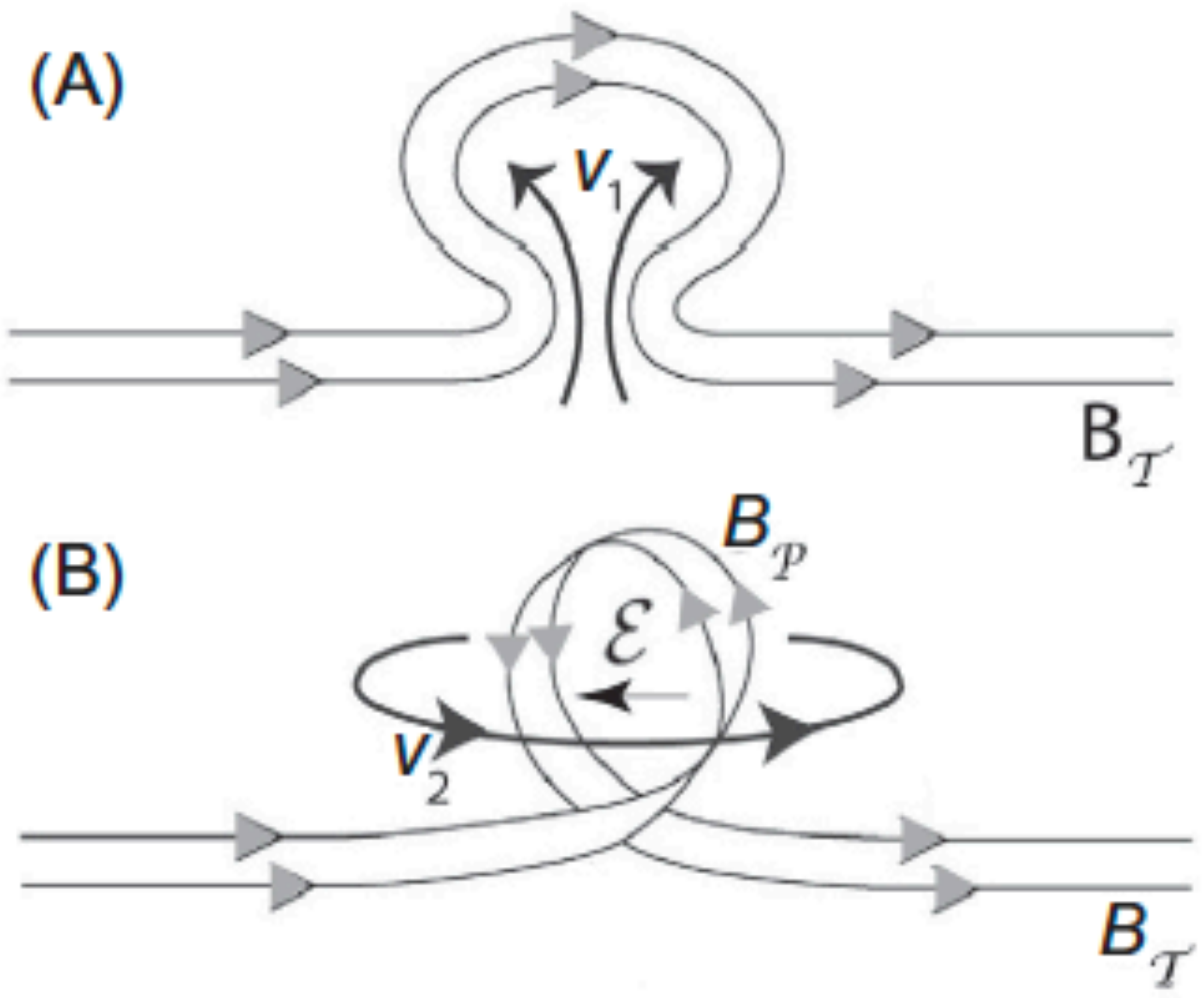

FIG. 3.21 Production of poloidal magnetic field $B_{\mathcal{P}}$ from a toroidal magnetic field $B_{\mathcal{T}}$ by a helical convective eddy. Flow in the eddy consists of two parts, a convective upwelling $\mathbf{v}_1$ in (A) and a quasigeostrophic circulation around the upwelling $\mathbf{v}_2$ in (B) with vorticity in the same direction as the upwelling, generating positive kinematic helicity. Positive helicity induces an e.m.f. $\mathcal{E}$ antiparallel to $B_{\mathcal{T}}$, and a loop of poloidal magnetic field with the polarity indicated by the *filled arrows*.

Helicity is defined as the correlation between the fluid velocity, $\mathbf{u}$, and its vorticity, $\nabla \times \mathbf{u}$:

$$H = \mathbf{u} \cdot \nabla \times \mathbf{u}$$

In an α^2 dynamo the α effect is parametrized as a linear relationship between the helicity induced emf and the toroidal field $\mathscr{E} = \overline{\mathbf{u} \times \mathbf{B}} = \alpha \mathbf{B_T}$

Both toroidal and poloidal magnetic fields are needed to make a self sustaining dynamo - for example

alpha-Ω model
Ω effect transforms large scale poloidal field into toroidal field

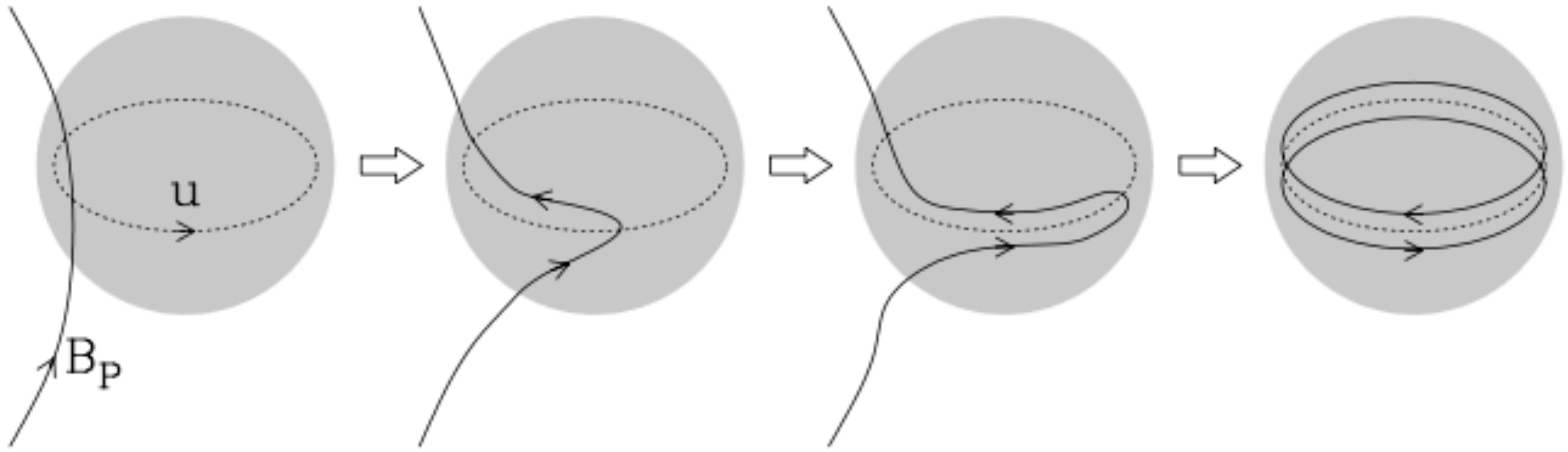

Equations governing core dynamics

- Ingredients of core dynamics

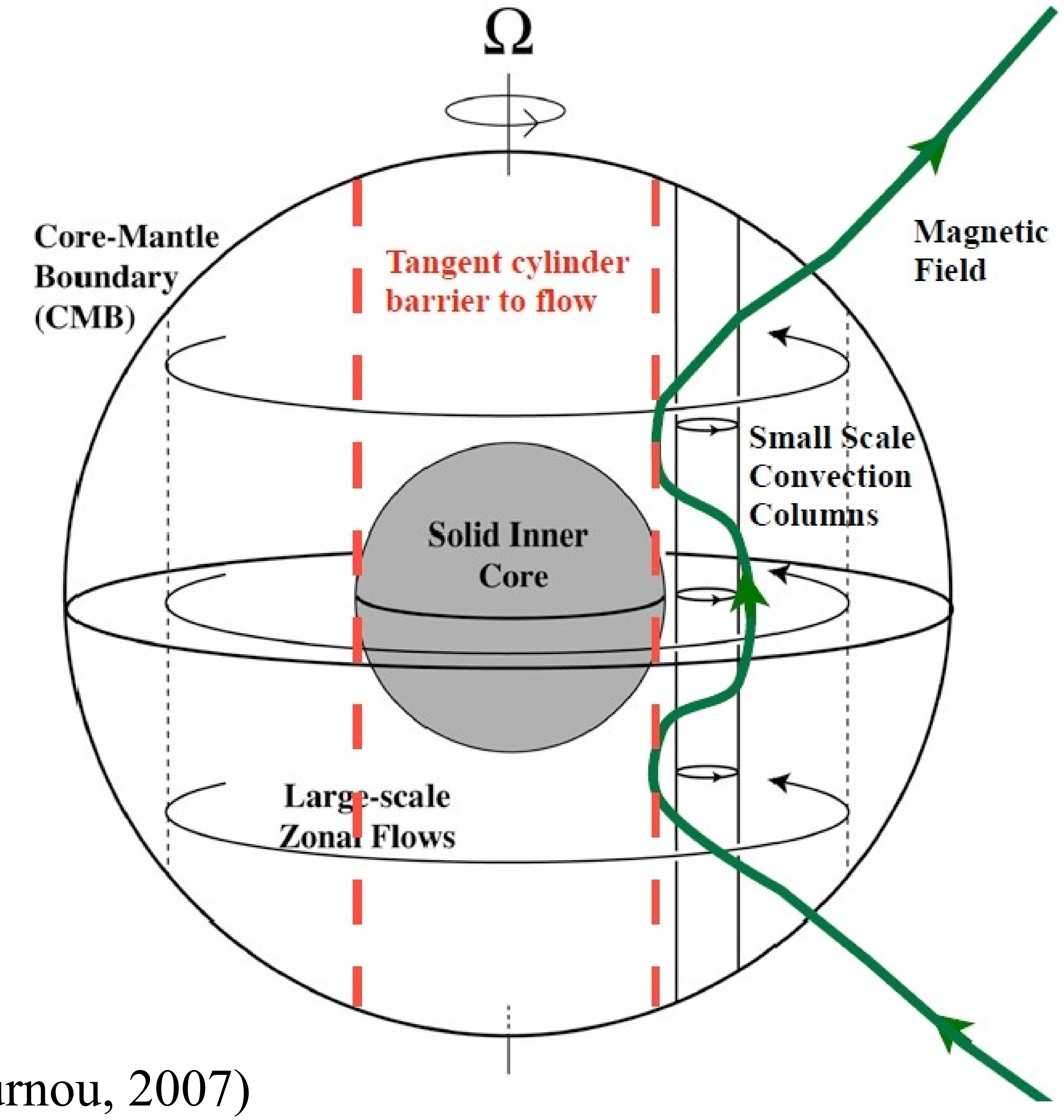

Not just the magnetic induction equation

(Modified from Aurnou, 2007)

Equations governing core dynamics

We start with

- The Navier-Stokes equation

$$\rho \frac{\partial \boldsymbol{u}}{\partial t} + \rho (\boldsymbol{u} \cdot \nabla) \boldsymbol{u} = -\nabla P + \rho \nu \nabla^2 \boldsymbol{u}$$

Rate of change of flow momentum w.r.t. time	Advection of flow momentum along with fluid	Force due to pressure gradient	Viscous force on fluid

But that's not all - there are more forcing terms

Equations governing core dynamics

- Adding rotation: The Coriolis Force

$$\rho \frac{\partial \boldsymbol{u}}{\partial t} + \rho(\boldsymbol{u} \cdot \nabla)\boldsymbol{u} + \boxed{2\rho(\boldsymbol{\Omega} \times \boldsymbol{u})} = \boxed{-\nabla P} + \rho \nu \nabla^2 \boldsymbol{u}$$

Coriolis force due to rotating reference frame

Centrifugal acceleration is added to pressure gradient, so P is effective pressure in the rotating frame.

Equations governing core dynamics

- The Buoyancy force

$$\rho_0 \frac{\partial \boldsymbol{u}}{\partial t} + \rho_0 (\boldsymbol{u} \cdot \nabla) \boldsymbol{u} + 2\rho_0 (\boldsymbol{\Omega} \times \boldsymbol{u}) = -\nabla P - \rho_0 \alpha T \boldsymbol{g} + \rho_0 \nu \nabla^2 \boldsymbol{u}$$

Temperature differences produce a change in density and so a buoyancy force.

- The effects of the buoyancy forces are most easily taken into account using the Boussinesq Approximation:

- The fluid is assumed to have constant background density ρ_0 with a background temperature field T_0, and perturbations T evolving as:

$$\frac{\partial T}{\partial t} + (\boldsymbol{u} \cdot \nabla) T_0 = \kappa \nabla^2 T$$

- Viscous and Ohmic heating effects neglected.
- Only dynamic effect of T is through gravity $\boldsymbol{g}$ acting on density perturbations $\rho \alpha T$ as described in the buoyancy force.

Equations governing core dynamics

- The Lorentz force

$$\rho_0 \frac{\partial \boldsymbol{u}}{\partial t} + \rho_0 (\boldsymbol{u} \cdot \nabla) \boldsymbol{u} + 2\rho_0 (\boldsymbol{\Omega} \times \boldsymbol{u}) = -\nabla P - \rho_0 \alpha T \, \boldsymbol{g} + \boxed{(\boldsymbol{J} \times \boldsymbol{B})} + \rho_0 \nu \nabla^2 \boldsymbol{u}$$

Lorentz force:
Force due to magnetic field acting on electric currents in fluid.

Equations governing core dynamics

- These are the equations of convection-driven, rotating magnetohydrodynamics under the Boussinesq approx.

$$\rho_0 \frac{\partial \boldsymbol{u}}{\partial t} + \rho_0 (\boldsymbol{u} \cdot \nabla) \boldsymbol{u} + 2 \rho_0 (\boldsymbol{\Omega} \times \boldsymbol{u}) = -\nabla P - \rho_0 \alpha T \boldsymbol{g} + (\boldsymbol{J} \times \boldsymbol{B}) + \rho_0 \nu \nabla^2 \boldsymbol{u}$$

$$\frac{\partial T}{\partial t} + (\boldsymbol{u} \cdot \nabla) T_0 = \kappa \nabla^2 T$$

$$\frac{\partial B}{\partial t} = \nabla \times (\boldsymbol{u} \times \boldsymbol{B}) + \eta \nabla^2 \boldsymbol{B}$$

$$\nabla \cdot \boldsymbol{u} = 0$$

$$\nabla \cdot \boldsymbol{B} = 0$$

These equations are used in numerical dynamo simulations…… usually they are non-dimensionalized first.

Dynamo Simulations: Pros

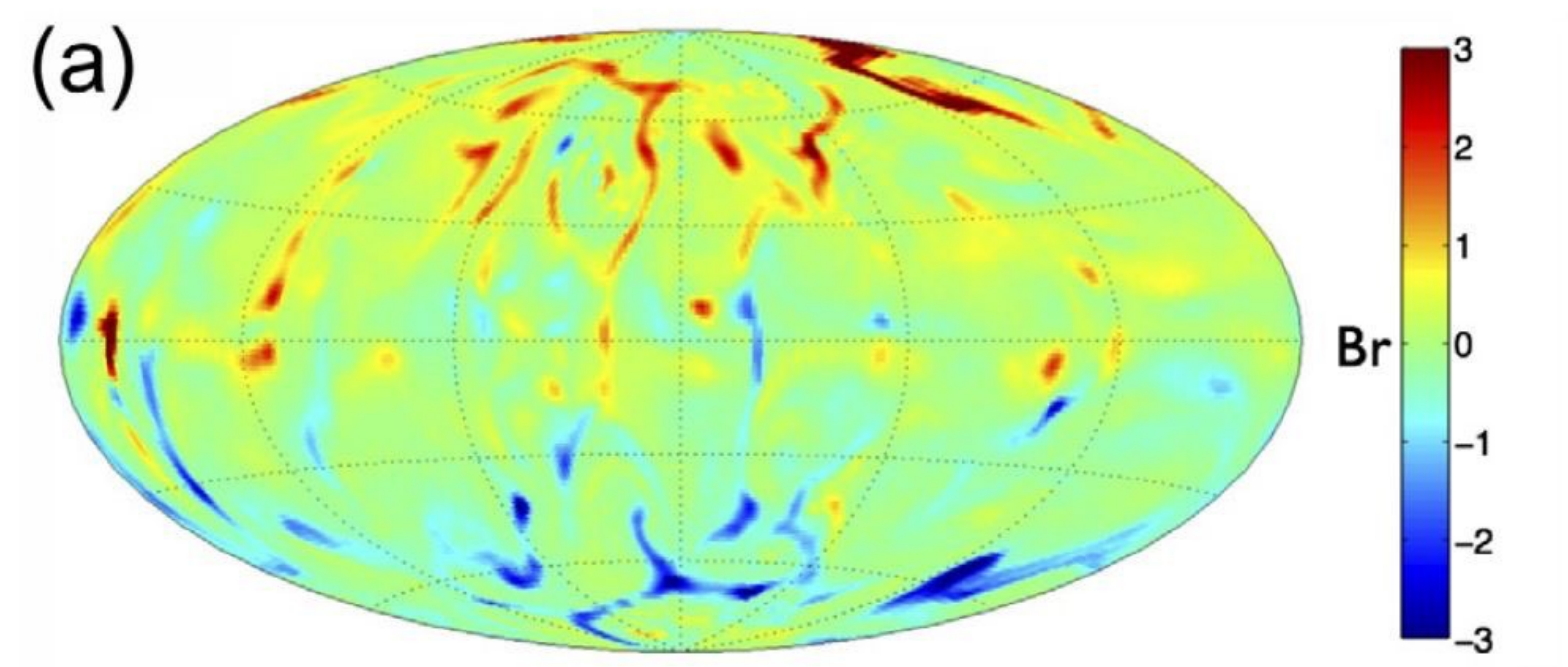

Radial magnetic field, core-mantle boundary
(snapshot)

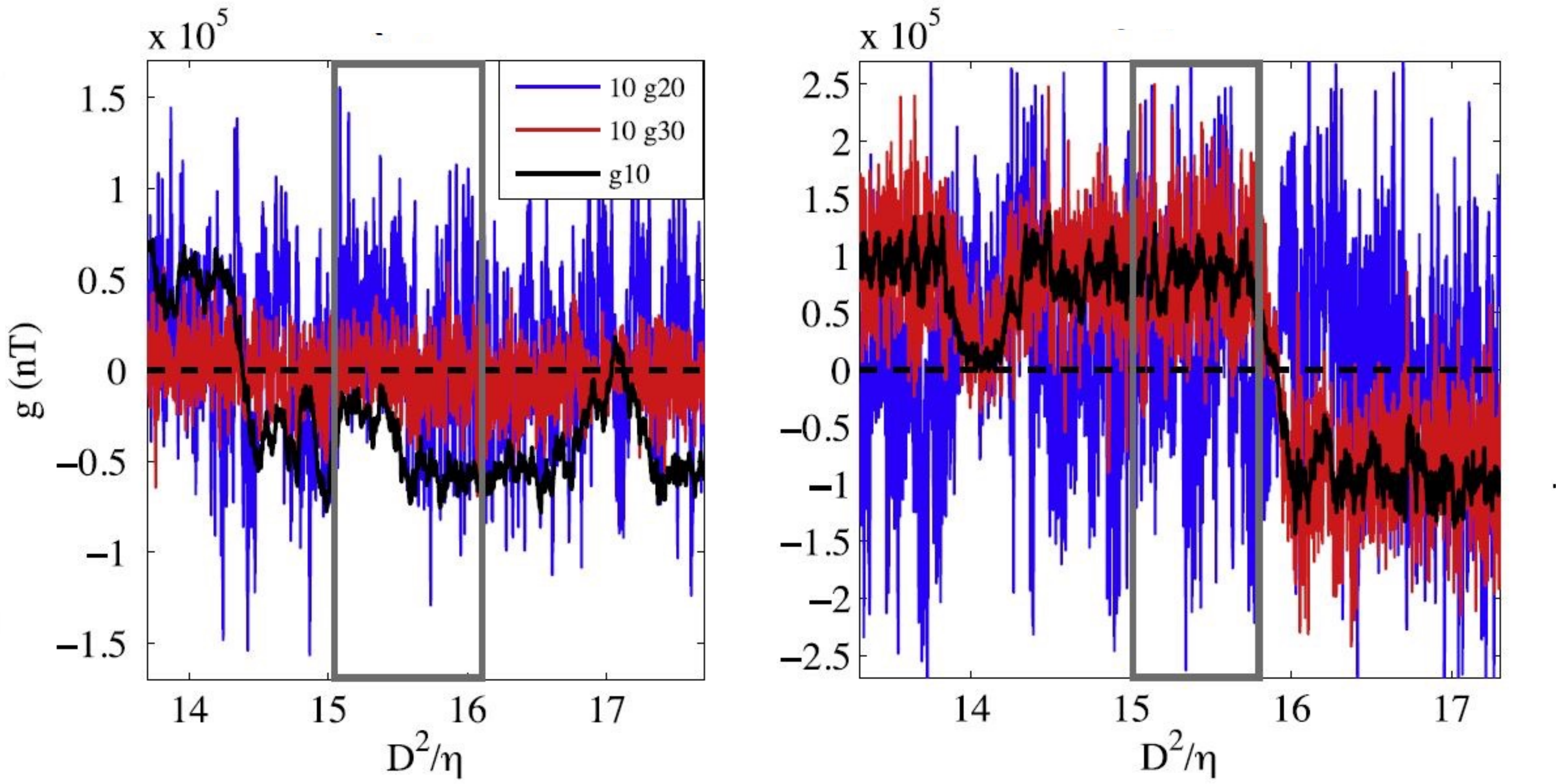

Heimpel and Evans (2013)

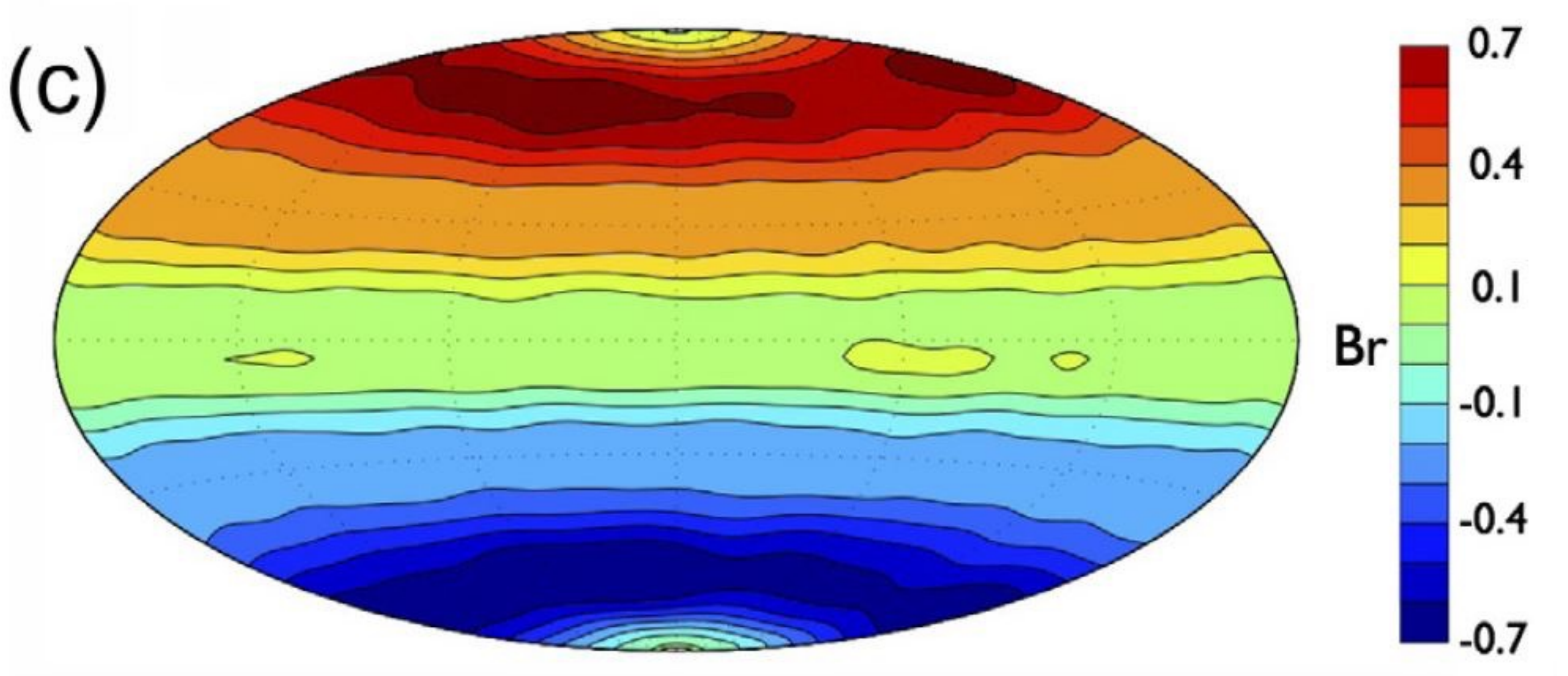

Radial magnetic field, core-mantle boundary
(time-average)

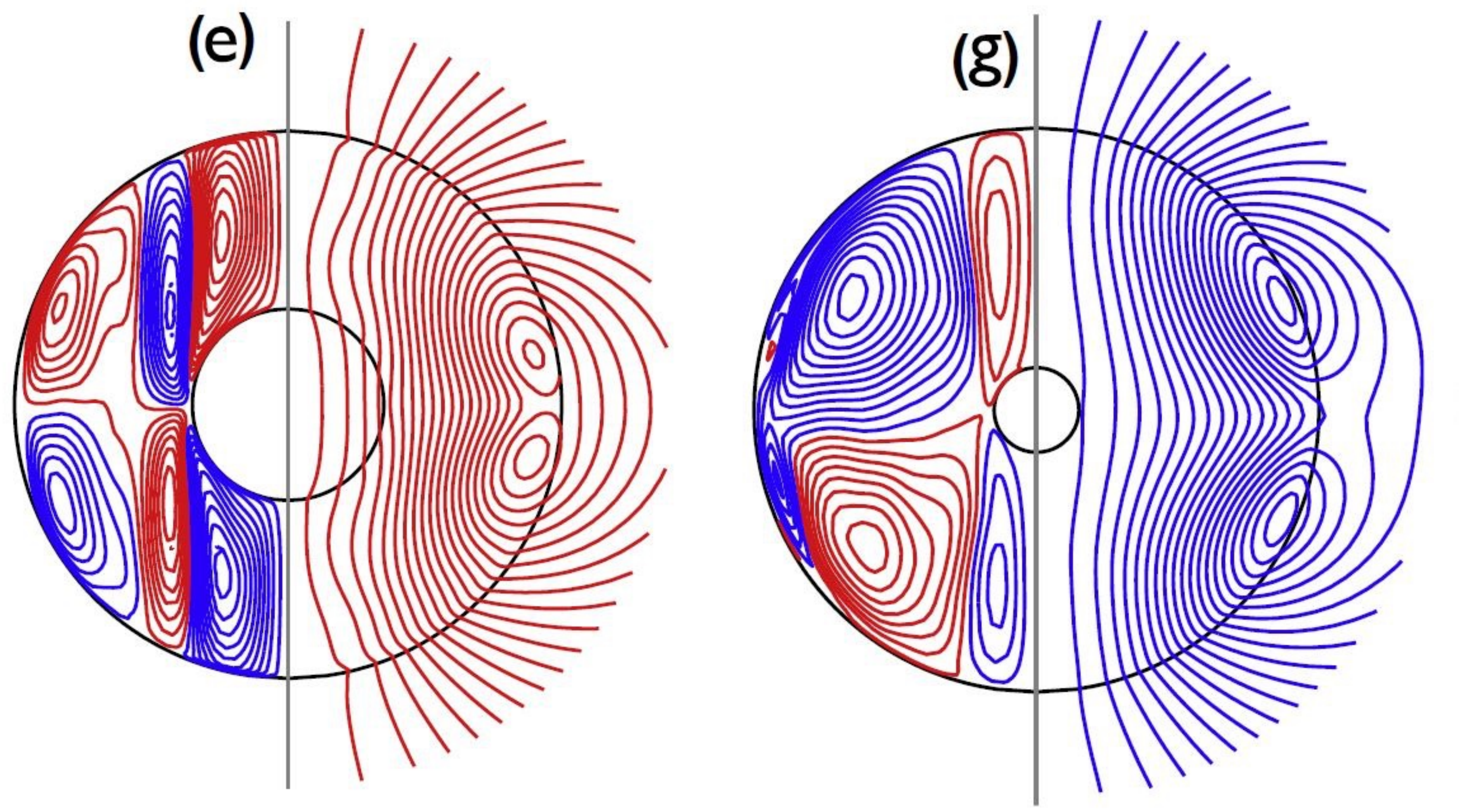

We get: ***B*** inside core; high spatio-temporal resolution; predictive power

Dynamo Simulations: Cons

Navier Stokes Eq'n

$$\frac{E}{Pm}\frac{D\boldsymbol{u}}{Dt} + \hat{\boldsymbol{z}} \times \boldsymbol{u} = -\nabla\tilde{P} + \frac{PmERa}{Pr}T'\hat{\boldsymbol{r}} + (\nabla \times \boldsymbol{B}) \times \boldsymbol{B} + E\nabla^2\boldsymbol{u}$$

Temperature Eq'n

$$\frac{\partial T'}{\partial t} + (\boldsymbol{u}\cdot\nabla)T' = \frac{Pm}{Pr}\nabla^2 T' + S$$

Magnetic Induction Eq'n

$$\frac{\partial \boldsymbol{B}}{\partial t} + (\boldsymbol{u}\cdot\nabla)\boldsymbol{B} = (\mathbf{B}\cdot\nabla)\mathbf{u} + \nabla^2\boldsymbol{B}$$

$$\nabla\cdot\boldsymbol{u} = \nabla\cdot\boldsymbol{B} = 0$$

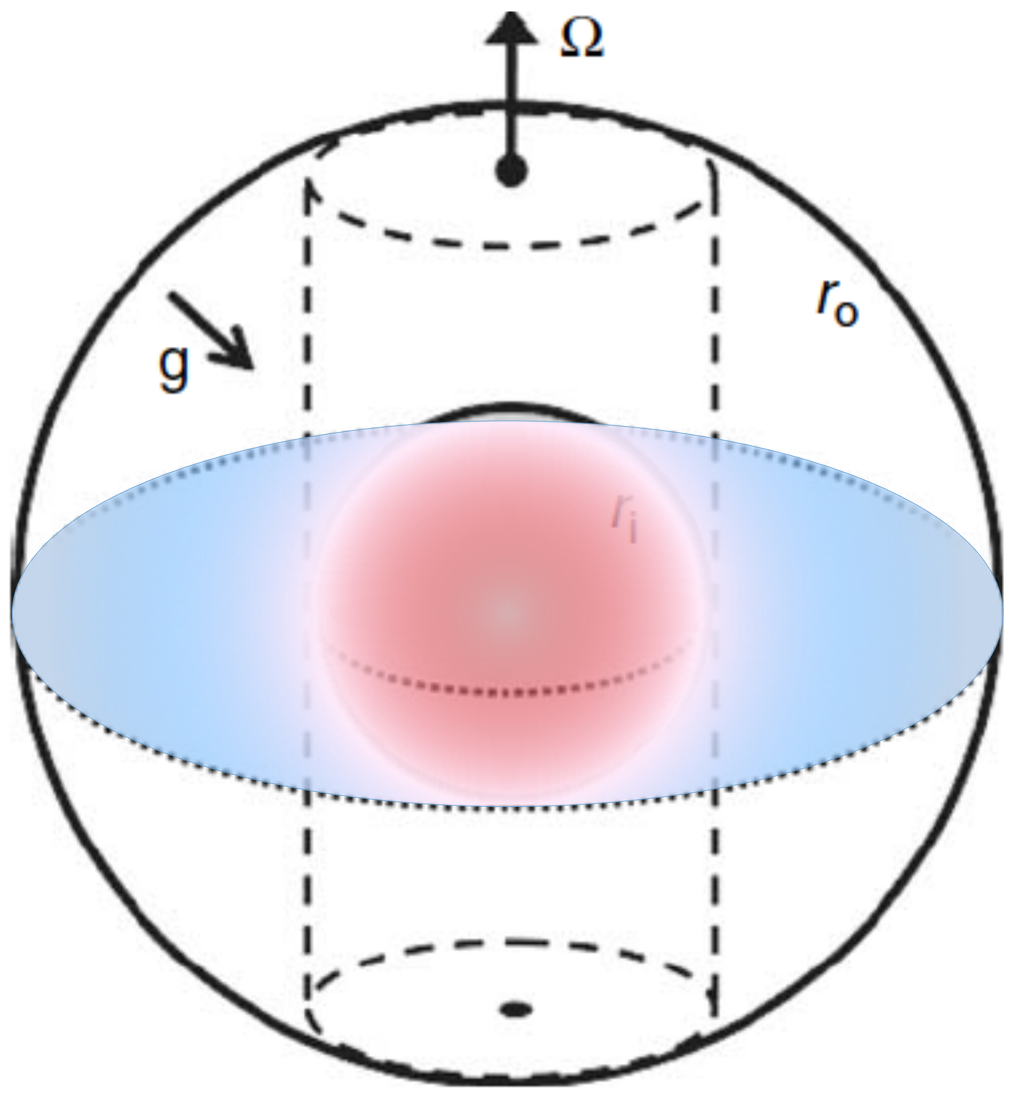

$\boldsymbol{B}$ = magnetic induction

$\boldsymbol{u}$ = velocity field

T = temperature

Dimensionless Numbers:
E = Ekman number; Pr = Prandtl number; Ra = Rayleigh number; Pm = Magnetic Prandtl number

Dynamo Simulations: Cons

$$\frac{E}{Pm}\frac{D\boldsymbol{u}}{Dt} + \hat{\boldsymbol{z}} \times \boldsymbol{u} = -\nabla\tilde{P} + \frac{PmERa}{Pr}T'\hat{\boldsymbol{r}} + (\nabla \times \boldsymbol{B}) \times \boldsymbol{B} + E\nabla^2\boldsymbol{u}$$

$$E = \frac{\text{Viscosity}}{\text{Rotation}} \sim 10^{-15} \qquad Ra = \frac{\text{Buoyancy}}{\text{Diffusion}} \sim 10^{30} \qquad Pm = \frac{\nu}{\eta} \sim 10^{-6}$$

- Parameters are far from geophysical reality

  (Note Pm ~ 1 in figure to right)
- Initial conditions are generally arbitrary
- Outputs are dimensionless and need to be rescaled

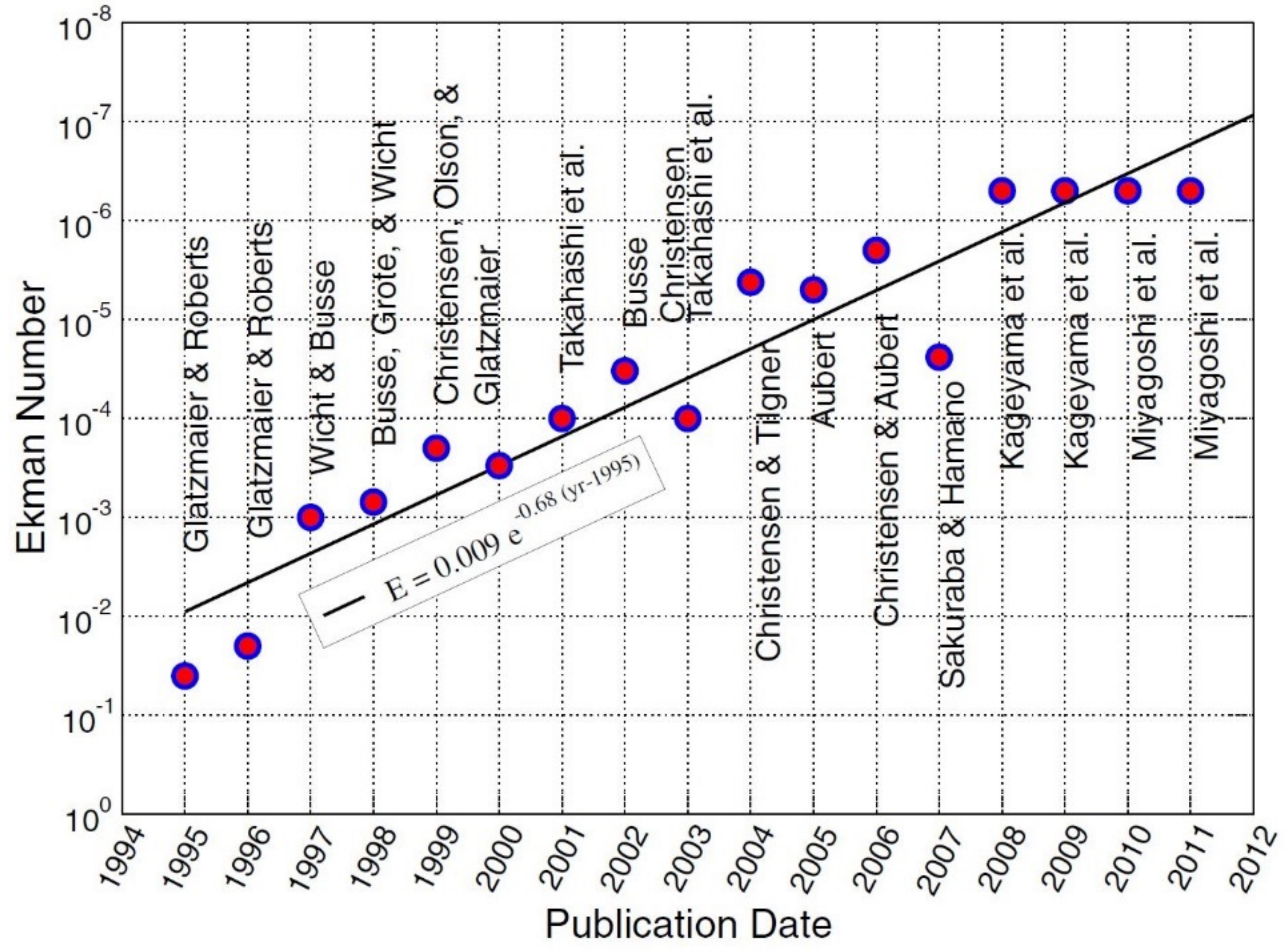

Roberts and King (2013)

Dynamo simulations are sometimes initialized with states considered representative of the geomagnetic field.

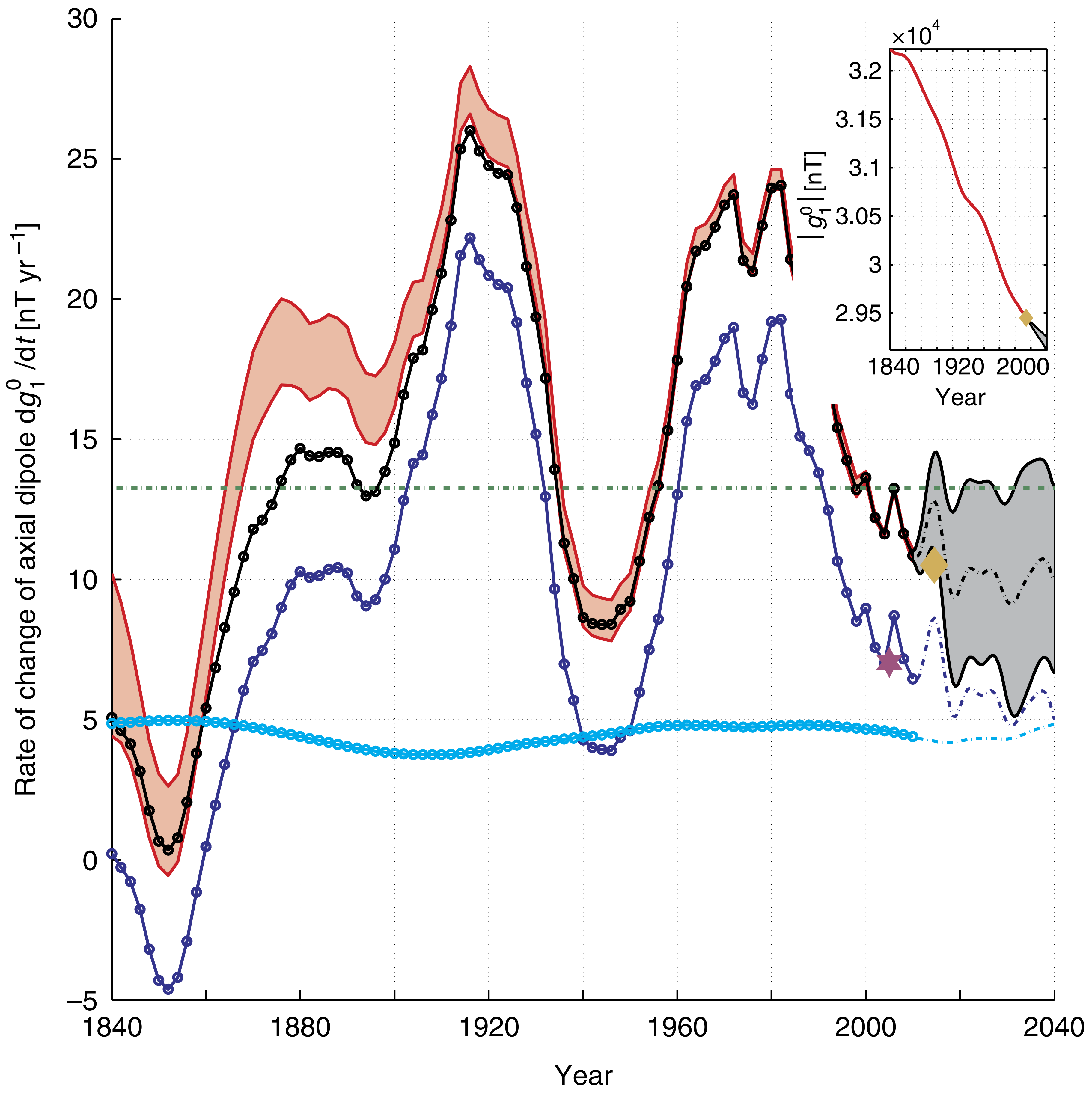

Figure 1 | Observed and modelled decay of the geomagnetic axial dipole. Axial dipole magnitude $|g_1^0|$ since 1840 (inset, red line, units: nT) and its rate of decay dg_1^0/dt (red shaded area shows one standard deviation uncertainties, units: nTyr^{-1}), from the COV-OBS[6] geomagnetic field reconstruction. Comparable dipole decay rates are produced by a prototype gyre acting on an asymmetric field (green dot-dashed line, see also Fig. 2a), and by a more realistic filtered gyre flow, acting on the observed field averaged over 2000–2010 (purple star, see also Methods section and Fig. 2c). The solid black line with dots is the retrieved axial dipole decay rate from a series of 3D inversions for the field and flow within the core, based on geodynamo model multivariate statistics[22] (see also Methods section and Figs 3 and 4). Each dot represents an independent inversion for the core state; these inversions are equally spaced in time. For the 3D inversion results, the dipole decay rate can be decomposed into its advective (dark blue line with dots) and diffusive (light blue line with dots) components. The grey area shows the 1 s.d. spread of an ensemble of 40 geodynamo model forward calculations, initialized using the estimated core state[22] in 2010, with randomized realizations of small scales; the ensemble mean is shown by the black dot-dash line. Corresponding ensemble mean advective and diffusive contributions are given by the dark and light blue dot-dashed lines. The latest values for the axial dipole and its decay rate in 2014, as determined using the data from ESA's Swarm satellite constellation[39], are marked by the gold diamonds.

Finlay et al., 2016, https://www.nature.com/articles/ncomms10422

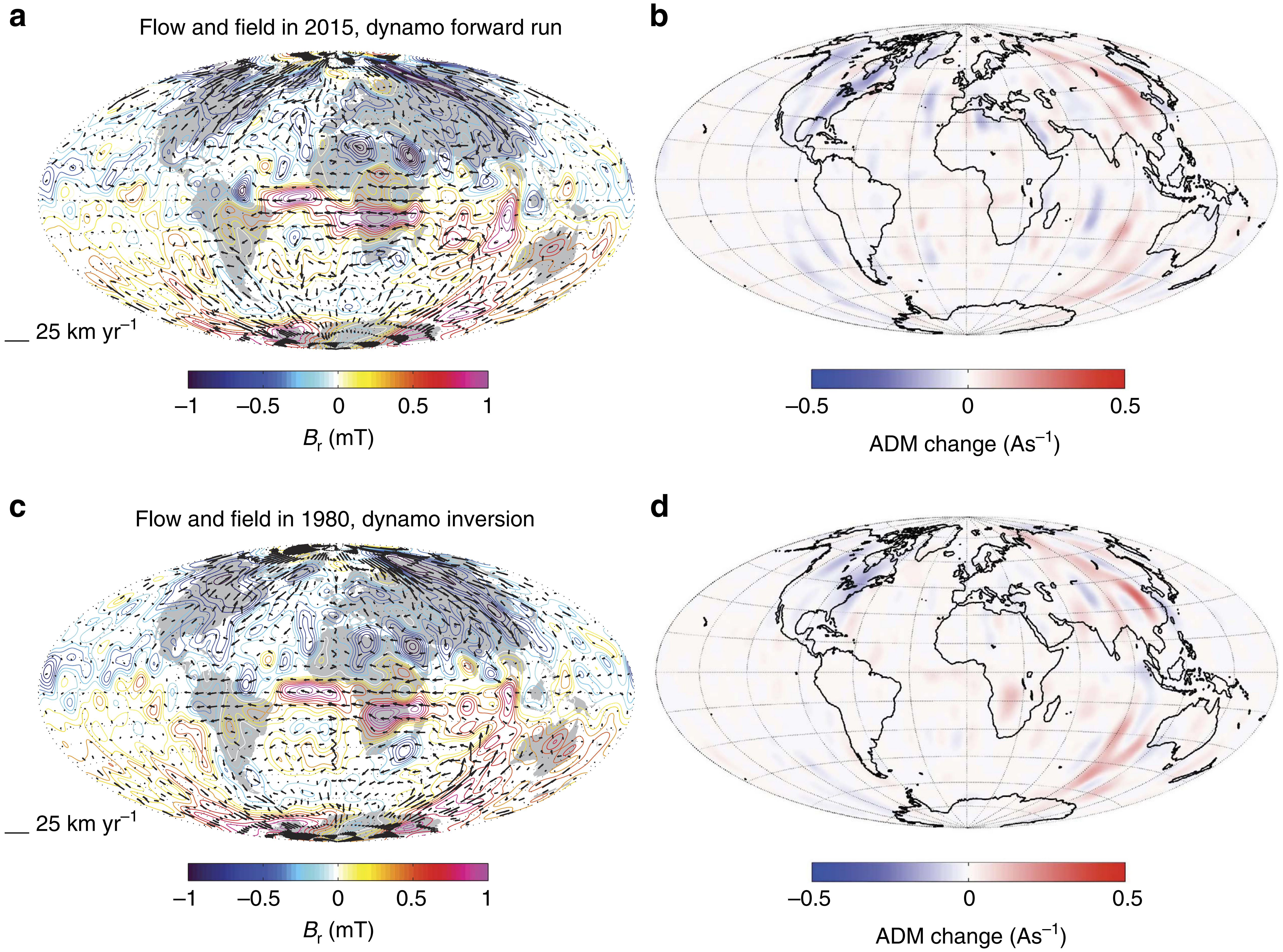

Figure 4 | Gyre-driven dipole decay as inferred using the CE dynamo. Maps of the core surface showing (**a**,**c**) core surface flow (arrows) acting on the radial magnetic field B_r (units: mT) and (**b**,**d**) the associated maps of contributions to axial dipole moment (ADM) change from core surface meridional flux transport $-3/2\mu_0\ u_\theta \sin\theta B_r$, units As^{-1}. (**a**,**b**) Here the situation in 2015 is shown, for the same 3D state presented in Fig. 3, derived from a forward run of the CE dynamo model[31] estimated from the inverted core state[22] in 2010. (**c**,**d**) The same quantities for the inverted 3D core state in 1980 are shown, when the magnitude of dipole decay was twice as large as in 2015. Note that magnetic diffusion has been taken into account when deriving the flows presented here, which was not the case for the results presented in Fig. 2.

Finlay et al., 2016, https://www.nature.com/articles/ncomms10422

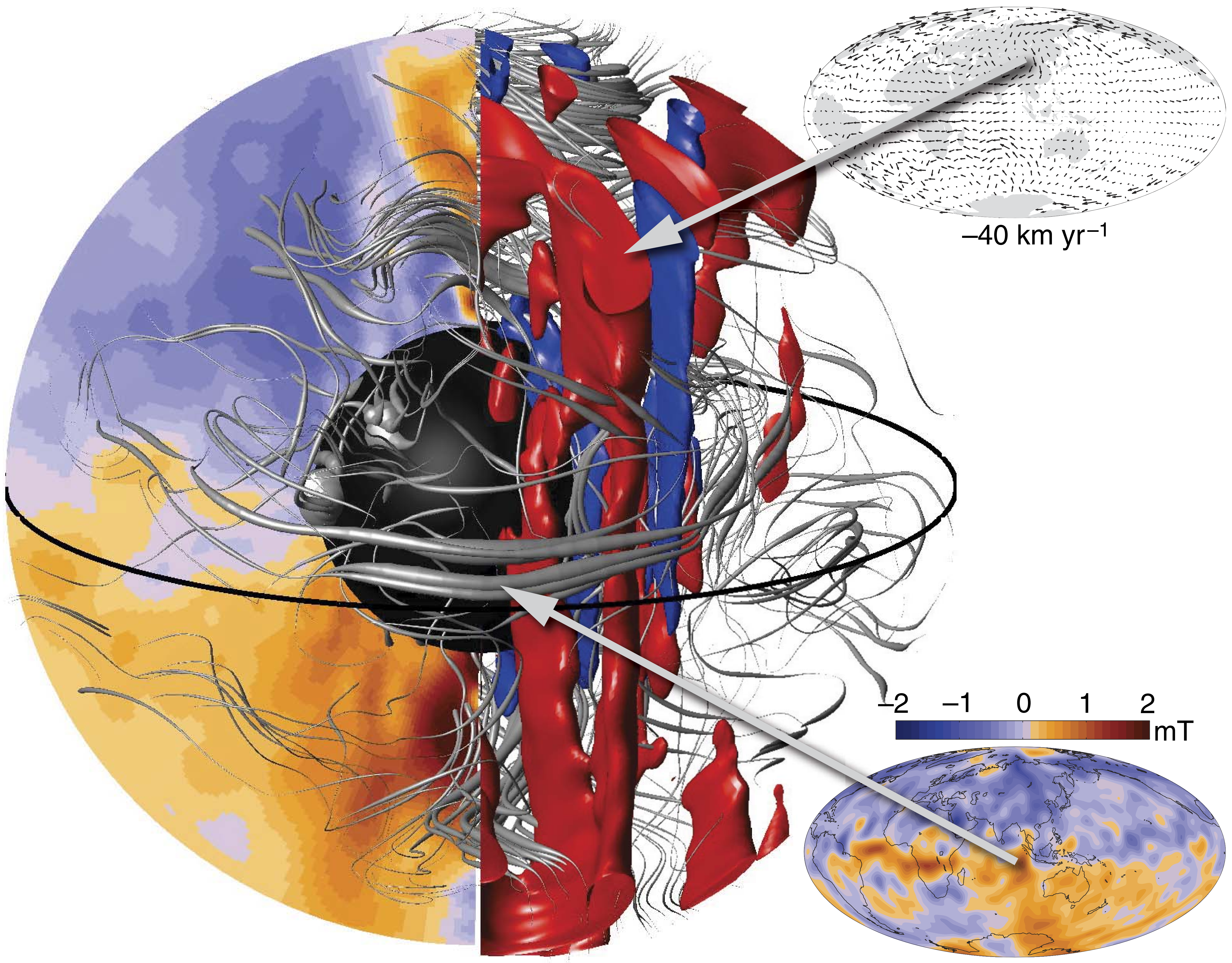

Figure 3 | Estimated field and flow within the core in 2015. Volume visualization of the estimated magnetic field and flow within Earth's core in 2015 from a numerical geodynamo[31] model forward run initialized with an inferred core state[22] for 2010. Orange and blue contours show the intensity of the radial magnetic field, azimuthally averaged in a meridional plane within the shell, and at the core surface in the inset. The red and dark blue iso-surfaces are of constant axial flow velocity and illustrate intense columnar convection at the eastern meridional limb of the gyre, as also seen in the inset core surface flow plot. Field lines within the shell have thickness proportional to their magnetic energy. The inner core is black and the core–mantle boundary is transparent. The 3D view faces longitude 90° E, with a cutaway between 90° and 180° E.

Finlay et al., 2016, https://www.nature.com/articles/ncomms10422